

This article was downloaded by:

On: 19 January 2011

Access details: *Access Details: Free Access*

Publisher *Taylor & Francis*

Informa Ltd Registered in England and Wales Registered Number: 1072954 Registered office: Mortimer House, 37-41 Mortimer Street, London W1T 3JH, UK



## International Journal of Polymeric Materials

Publication details, including instructions for authors and subscription information:

<http://www.informaworld.com/smpp/title~content=t713647664>

### Long Spacing in Polyblock Poly(ether ester)s—Origin and Peculiarities

S. Fakirov<sup>a</sup>; A. A. Apostolov<sup>a</sup>; C. Fakirov<sup>ab</sup>

<sup>a</sup> Laboratory on Structure and Properties of Polymers, Sofia University, Sofia, Bulgaria <sup>b</sup> Max-Planck-Institut fuer Polymerforschung, Mainz, Germany

**To cite this Article** Fakirov, S. , Apostolov, A. A. and Fakirov, C.(1992) 'Long Spacing in Polyblock Poly(ether ester)s—Origin and Peculiarities', *International Journal of Polymeric Materials*, 18: 1, 51 — 70

**To link to this Article:** DOI: 10.1080/00914039208034813

**URL:** <http://dx.doi.org/10.1080/00914039208034813>

PLEASE SCROLL DOWN FOR ARTICLE

Full terms and conditions of use: <http://www.informaworld.com/terms-and-conditions-of-access.pdf>

This article may be used for research, teaching and private study purposes. Any substantial or systematic reproduction, re-distribution, re-selling, loan or sub-licensing, systematic supply or distribution in any form to anyone is expressly forbidden.

The publisher does not give any warranty express or implied or make any representation that the contents will be complete or accurate or up to date. The accuracy of any instructions, formulae and drug doses should be independently verified with primary sources. The publisher shall not be liable for any loss, actions, claims, proceedings, demand or costs or damages whatsoever or howsoever caused arising directly or indirectly in connection with or arising out of the use of this material.

*Intern. J. Polymeric Mater.*, 1992, Vol. 18, pp. 51–70  
Reprints available directly from the publisher  
Photocopying permitted by license only  
© 1992 Gordon and Breach Science Publishers S.A.  
Printed in Great Britain

# Long Spacing in Polyblock Poly(ether ester)s—Origin and Peculiarities

S. FAKIROV, A. A. APOSTOLOV and C. FAKIROV†

*Laboratory on Structure and Properties of Polymers, Sofia University, 1126 Sofia, Bulgaria*

*(Received February 14, 1992)*

Poly(ether ester)s (PEE) based on poly(butylene terephthalate) (PBT) as hard segments and poly(ethylene glycols) (PEG) with different molecular weight as soft segments are studied by means of WAXS and SAXS in the drawn and undrawn state after annealing at various temperatures ( $T_a$ ). The repeatedly reported strong increase of the long spacing  $L$  with  $T_a$  is confirmed once again. In the same time the directly measured by WAXS crystallite size of PBT remains insensitive to  $T_a$  and the increase of  $L$  with  $T_a$  is the stronger, the higher the PEG content. It is concluded therefore that the rise in  $L$  is due to the expansion of the amorphous intercrystalline layers rather than to crystal thickening, the latter being the case of semicrystalline homopolymers.

The observed much stronger increase of  $L$  with  $T_a$  in undrawn samples than in drawn ones is explained by melting of less perfect crystallites at higher  $T_a$  and dephasing processes in the amorphous regions. The conclusions drawn seem to be valid for other segmented polyblock copolymers and suggest some specific features of the block copolymers in comparison to homopolymers.

**KEY WORDS** Thermoplastic elastomers, SAXS, long spacing, crystallite size, crystal thickening.

## INTRODUCTION

Thermoplastic elastomers are now of great commercial importance as engineering-type materials because of their extraordinary combination of elasticity, toughness, low temperature flexibility and strength at 150°C. This set of properties is related mainly to the existence of cross-links tying the array of macromolecules into an infinite network. In natural rubber and synthetic elastomers these cross-links represent chemical bonds. In thermoplastic elastomers they are replaced by glassy, crystalline or even hydrogen-bonded molecules or ionic associations.<sup>1</sup>

In order to behave as a thermoplastic elastomer the molecules must contain two types of units, blocks or chain segments: amorphous type (above  $T_g$ ) referred to as soft segments or blocks and hard segments or blocks. The soft segments impart elastomeric character to the copolymer while the hard blocks are capable of intermolecular association with other hard blocks; they should form a solid phase within a desired temperature range in order to impart dimension stability to the

†Current address: Max-Planck-Institut fuer Polymerforschung, Ackermannweg 10, 6500 Mainz, Germany.

array of molecules. At high temperature, dissociation of the physical bonds occurs. In order to insure the formation of a three-dimensional network, each molecule should contain at least two hard blocks. The soft and hard blocks may be arranged in various ways, randomized or ordered. Their way of ordering affects the physical and mechanical properties of the material.<sup>1</sup>

Thermoplastic elastomers are attractive subjects for structural investigations not only because of their peculiar mechanical properties but also since they offer many modeling opportunities due to their crystallization ability, multiblock character and possibility of varying both the block flexibility and length. There are also a lot of unanswered questions concerning the deformation mechanism, the response to thermal treatment with respect to the long spacing, etc.

Small angle x-ray scattering (SAXS) studies of numerous homopolymers showed a strong increase of the long spacing  $L$  with the rise of the crystallization temperature. This observation is explained by the phenomenon of crystal thickening representing a rise of the crystalline lamellae size with crystallization temperature.<sup>2</sup> This is established for a good deal of homopolymers crystallized from both solutions and melts.<sup>2</sup> It is important to note that  $L$  of solution grown polyethylene crystal mat increases five times (from 100 Å to 500 Å) when the annealing temperature  $T_a$  increases from 70 up to 135°C.<sup>2</sup> For the melt-crystallized and 17 times drawn polyethylene  $L$  doubles its value (from 200 Å to 400 Å).<sup>2</sup> Poly(ethylene terephthalate) (PET) shows a rather similar behavior in the annealing range between 100 and 260°C—for undrawn samples  $L$  increases from 132 up to 295 Å while for drawn ones this rise is from 110 up to 255 Å.<sup>3</sup>  $L$  rises from 100 up to 145 Å in the case of drawn poly(butylene terephthalate) (PBT).<sup>4</sup>

Segmented block copolyesters for which the long spacing  $L$  was determined by SAXS<sup>5-7</sup> behave in the same manner.  $L$  is assumed to be again the distance between the crystalline lamellae, i.e. the sum of the lamella thickness and that of the amorphous region between the lamellae.<sup>8</sup> The observed substantial increase in  $L$  regardless of the polymer composition is explained again by thickening of the lamellae.<sup>8,9</sup> The same explanation of the observed rise in the  $L$ -values as a result of annealing at increasing temperatures is adopted by Miller and Cooper who investigated the chain conformation in block copoly(ether ester)s by small angle neutron scattering.<sup>10</sup>

Wegner *et al.*<sup>7,11</sup> observed an isotropic distribution of the hard segment crystallites in thermoplastic poly(ether ester)s based on PBT and poly(tetramethylene oxide) (PTMO) quenched from the melt. When the same samples are subjected to annealing, an exponential increase in the long spacing is found. The authors note further that in view of the rather short average sequence length of the hard segments (the number average degree of polymerization for the three samples studied is 4.8, 6.3 and 12.5, respectively), it is very surprising to see that long spacings of up to 250 Å are easily reached and that neither hard nor soft segment length seems to influence the annealing behavior in terms of the expected long spacing when the supercooling ( $\Delta T = T_m - T_a$ ) is chosen as the relevant thermodynamic parameter. Furthermore, a number of peculiarities are emphasized<sup>11</sup>: (i) much higher  $L$ -values can be reached for all samples; (ii) the samples differing by their hard segment block length differ strongly in their long spacings which can be reached at a fixed

value of  $\Delta T$ . At a given  $\Delta T$   $L$  increases with the rise of the amount of soft segments, i.e. inversely to the average length of the hard segment blocks. The same observation is reported by Adams and Hoeschele<sup>8</sup>—in rapidly cooled samples the long spacing is substantially constant at about 130 Å for hard copolyesters containing more than 50 wt.% PBT units;  $L$  increases for softer copolymers: up to about 200 Å in the case when the concentration of PBT units is decreasing towards 10 wt.%.

The results described refer to thermoplastic poly(ether ester)s (PEE) based on PBT as hard segments and PTMO as soft segments. The same results are obtained with annealed drawn and undrawn PEE based also on PBT as hard segments but having poly(ethylene glycols) (PEG, molecular weight  $\bar{M}_n$  of 600, 1000 and 2000) as soft segments.<sup>12–15</sup> Again after annealing the undrawn samples attain doubly higher  $L$ -values than those of undrawn ones. The strongest increase of the long spacing is observed with the samples characterized by the lowest PBT content.<sup>14</sup>

Recently the effect of the block length of the same PEE samples on their deformation behavior was studied.<sup>16</sup> By comparison of DSC, WAXS and SAXS measurements it was concluded that the chain portions linking two adjacent lamellae comprise one hard  $l^h$  and two soft  $l^s$  segments, i.e.  $L^{\max} = l_c + 2l^s + l^h$  where  $l_c$  is the lamella thickness in the draw direction. In the thorough study by SAXS under stress and strain of drawn annealed PEE bristles<sup>17</sup> or bristles with destroyed and thereafter regenerated structure<sup>18</sup> an attempt was made to answer the question to what extent the concept of crystal thickening is applicable to block copolymers with limited crystallizable block length in order to explain the effect of annealing on the long spacing. It was assumed that the drastic increase in  $L$  after annealing is related to the formation of longer (than before annealing) interlamellar regions incorporating small and rather defective crystallites. The average density of these regions is higher than that of the amorphous areas but still below the increased density of the lamellae after annealing.<sup>18</sup>

Finally, an interesting observation related to the origin of the long spacing in PEE thermoplastic elastomers should be mentioned.<sup>5</sup> Surprisingly, the composition containing less than 10 wt.% PBT units yielded a SAXS peak even though there was no indication of crystallinity in the sample based on WAXS or density measurements. Perego *et al.*<sup>5</sup> assumed that some ordering in the amorphous phase of hard segments too short to crystallize may explain this observation.

In addition to this report, we also observed a long spacing increasing with the measuring temperature in PEE containing only 24 wt.% PBT, with almost no evidence of crystalline phase in the WAXS spectrum taken by synchrotron radiation.<sup>19</sup>

Literature data show so far considerable ambiguity concerning the origin and nature of the strong annealing dependence as well as the great difference in the  $L$ -values of drawn and undrawn samples of segmented block copolymers. The present study aims to answer these questions by means of direct measurements of both long spacings and crystallite sizes in drawn and undrawn annealed polyblock PEE differing in chemical composition and block length.

## EXPERIMENTAL

## Materials

The sample material represents polyblock PEE consisting of PBT as hard segments and PEG as soft segments in different ratios. The synthesis is carried out on a semicommercial scale as described in.<sup>12</sup> It should be noted that the starting PEG are characterized (according to GPC analysis) by a rather narrow molecular weight distribution ( $\bar{M}_w/\bar{M}_n = 1.30$ ). They are denoted as PEG 600, PEG 1000 and PEG 2000, although their weights are actually lower, as shown in Table I.

Calculations based on normal kinetics of polyester formation and <sup>1</sup>H NMR as well as <sup>13</sup>C NMR measurements<sup>12,13</sup> were used for the determination of the average degree of polymerization of the hard segments (Table I). Assuming a total molecular weight of the copolymer of about 20,000 (for products of technical interest

TABLE I  
Some Characteristics of the Samples

Sample designation	Composition (from the starting ratio) <sup>12,13</sup> (wt. %)		Degree of polymeriz. <sup>16</sup>		Average mol. wt. of PEG (from GPC) <sup>16</sup> $\bar{M}_n^1$	Segment length (from chem. comp.) <sup>16</sup> (Å)		Maximal melting temp. $T_m^{13,14,19}$ (°C)	Degree of cryst. (from DSC) <sup>13,16</sup> (%)	
	PBT	PEG	PBT	PEG		$l^h$	$l^s$		$w_c$	$w_c^{PBT}$
	100/0	100	0	—	—	—	—	—	230	—
75/25(1000)	75	25	13.8	20.2	890	160	71	212	30	40
49/51(1000)	49	51	4.4	20.2	890	51	71	188	13	27
24/76(1000)	24	76	1.4	20.2	890	16	71	—	—	—
67/33(600)	67	33	4.1	7.3	320	48	26	184	22	33
57/43(1000)	57	43	6.1	20.2	890	71	71	196	19	33
41/59(2000)	41	59	3.2	8.6/32	380/1400	37	30/112	198	13	31

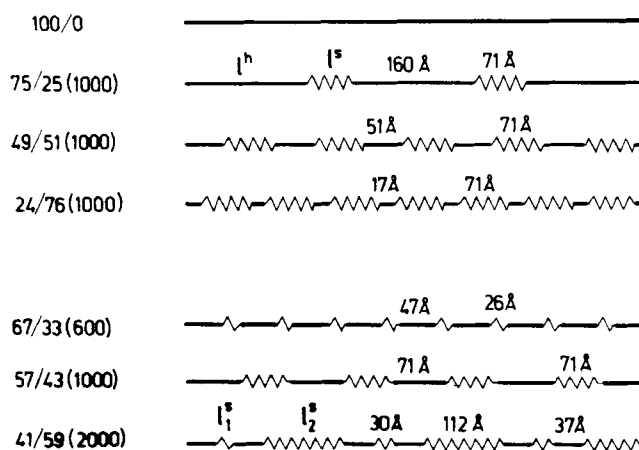


FIGURE 1 Schematic presentation of the poly(ether ester) polyblock extended macrochains;  $l^h$  and  $l^s$  are the lengths of the hard and soft segments, respectively; their values in Å are given.

it is of about  $2-4 \cdot 10^4$ ),<sup>9</sup> these data suggest an average total number of blocks in each macromolecule of about 20. For an extended chain conformation the average soft segment length  $l^s$  and the average length of the hard segments  $l^h$  were calculated (Table I) and presented schematically in Figure 1.

Bristles of diameter of about 1 mm were prepared by means of melt extrusion. These isotropic (according to WAXS measurements) bristles were drawn at room temperature on a Zwick 1464 machine with a cross-head speed of 5 mm/min until the entire sample undergoes neck formation which corresponds to a draw ratio  $l/l_0 = 5$ , where  $l_0$  and  $l$  are the length of the starting undrawn sample and after drawing, respectively. The drawn material exhibits a reversible deformation at room temperature of about 50%.

The drawn bristles (diameter of about 0.5 mm) as well as the undrawn ones were annealed with fixed ends in vacuum at various temperatures  $T_a$  for 6 h. All measurements were carried out with the samples thus treated.

### Methods

Some of the measurements were performed using an x-ray source with rotating anode and a pinhole collimation. The scattering patterns were registered by a two-dimensional position sensitive detector. The latter is filled with xenon and has a resolution of 0.2 mm in each direction. The two-dimensional scattering patterns consist of  $512 \times 512$  data points. Sample-to-detector distance was 80 cm. Calibration was made with Lupolen and with  $C_{36}H_{74}$  paraffin. Meridian cuts through the two-dimensional scattering pattern were calculated taking an average over 4 equatorial points. Each pixel corresponds to a detector element  $0.2 \times 0.2$  mm<sup>2</sup>.

The rest of the measurements were carried out using Ni-filtered Cu  $K_\alpha$ -radiation on a Kristalloflex (Siemens) x-ray generator equipped with wide- and small-angle (Kratky) diffractometer. Since only one bristle of diameter of about 0.5 mm was used, the collimation was considered as point-like and no desmearing of the SAXS data was made. Thus the long spacing  $L$  was directly calculated from the peak position of the small angle maximum using Bragg's law in the form

$$L = \frac{\lambda}{2\theta} \quad (1)$$

where  $\lambda = 1.54$  Å is the wavelength and  $2\theta$  is the scattering angle in radians.

The lamella thickness  $l_c$  in the drawn samples was obtained from the WAXS measurements as crystal size in the  $(\bar{1}04)$  direction since the plane  $(\bar{1}04)$  makes approximately 10 degrees with the "c" axis. The Scherrer equation was used

$$l_c = \frac{1.07\lambda}{\beta \cos \theta} \quad (2)$$

where  $\theta$  is the Bragg's angle. In order to achieve higher accuracy, the integral width  $\beta$  of  $(\bar{1}04)$  peak and corresponding value of the Scherrer constant 1.07 were taken.<sup>20</sup> The crystal size in the undrawn samples was determined in the same way using the  $(100)$ ,  $(010)$  and  $(\bar{1}04)$  reflections.

## RESULTS

Figures 2 and 3 show the WAXS and SAXS curves, respectively, taken with drawn and undrawn annealed PEE samples differing in chemical composition (PBT/PEG(1000) ratio). The crystallite sizes (from WAXS, Figure 2) and the long spacings (from SAXS, Figure 3) were calculated from these experimental curves. In the first case the lamella thickness  $l_c$  was actually determined using the  $(\bar{1}04)$  reflection; despite that the latter is a very weak one (Figure 2), it offers the advantage to provide some idea on the crystallite size changes in the direction of the long spacing.

The strongest  $(100)$  and  $(010)$ , Figure 2) reflections were chosen in addition to  $(\bar{1}04)$  for the study of the undrawn samples since an isotropic distribution of hard segment crystallites has been reported.<sup>11</sup> The crystallite size and the long spacing obtained are plotted in Figures 4 and 5 for drawn and undrawn samples, respectively.

The well known and repeatedly reported<sup>1-14</sup> dependence of  $L$  on the annealing temperature can be observed and at least two peculiarities should be noted: (i) the  $L$ -values of undrawn samples are again higher than those of drawn ones having

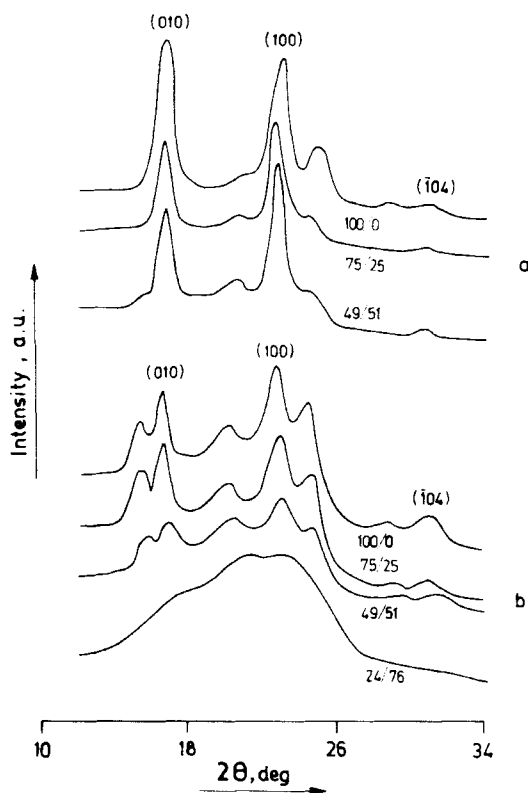


FIGURE 2 WAXS curves of drawn (a) and undrawn (b) PBT and PEE annealed at  $T_a = 170^\circ\text{C}$  for 6 hrs in vacuum except the sample 24/76 which is unannealed; the figures to the curves refer to the PBT/PEG(1000) ratio in wt. %.

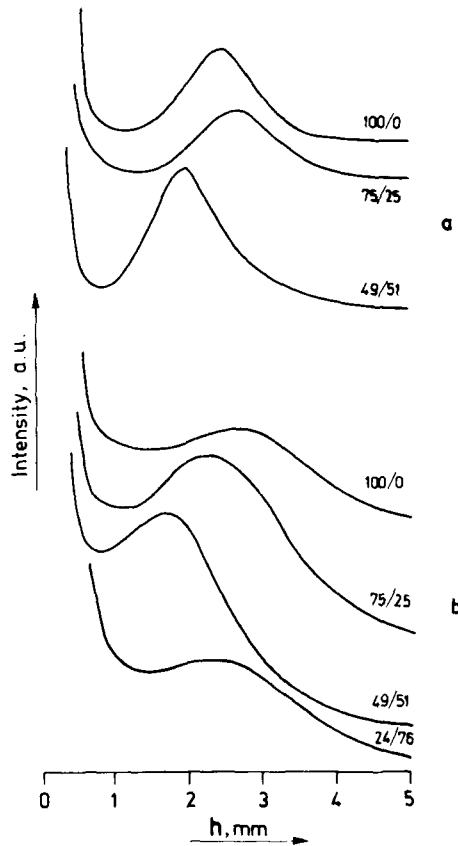


FIGURE 3 SAXS curves of drawn (a) and undrawn (b) PBT and PEE annealed at  $T_a = 170^\circ\text{C}$  for 6 hrs in vacuum except the sample 24/76 which is unannealed; the figures to the curves refer to the PBT/PEG(1000) ratio in wt. %.

the same chemical composition (Figures 4 and 5, respectively) and (ii) the rise of the soft segment content results in a strong increase of  $L$ , as observed previously.<sup>11,14</sup> In the case of sample 24/76 (1000) which is almost free of crystalline phase (Figure 2b) the  $L$ -values (Figure 5a) are even higher than the maximum ones for pure drawn PBT annealed at the most favorable temperature (Figure 4).

The crystallite sizes  $l_c$  measured in the draw direction ( $D_{104}$ , Figure 4b) keeps an almost constant value of about  $50 \text{ \AA}$  regardless of the annealing temperature. From the runs of the plots for  $L$  and  $l_c$  (a and b in Figure 4, respectively) one can conclude that the difference  $L - l_c = l_a$  increases slowly at low  $T_a$ -values but becomes significant at  $T_a$  close to the melting temperature  $T_m$ , particularly for samples with higher soft segment content. Since the value of  $l_a$  provides an idea about the dimensions of the non-crystalline interlamellar regions in the orientation direction, an assumption can be made that the increase of  $L$  with the rise of  $T_a$  can be hardly due to lamella thickening since  $l_c$  remains constant. This assumption is supported by other observations as disclosed below.

Rather similar is the situation with undrawn samples where the described effects



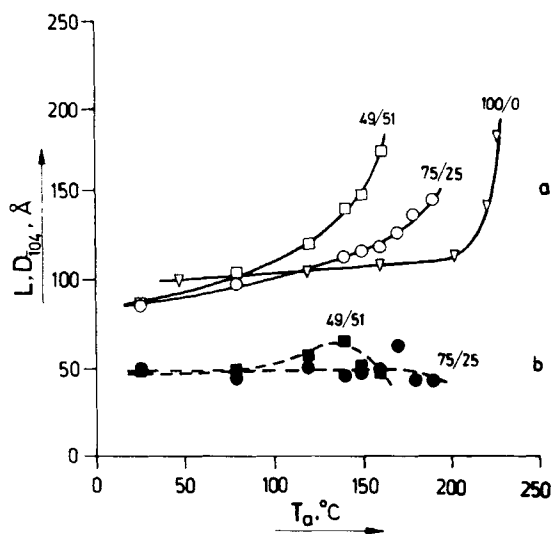


FIGURE 4 Effect of the annealing temperature  $T_a$  on the long spacing  $L$  (a) and crystallite sizes  $D_{104}$  (b) for drawn PBT and PEE with various PBT/PEG(1000) ratios (wt.%): ( $\square$ ) -  $L$  of 49/51, ( $\circ$ ) -  $L$  of 75/25, ( $\nabla$ ) -  $L$  of 100/0, ( $\blacksquare$ ) -  $D_{104}$  of 49/51, ( $\bullet$ ) -  $D_{104}$  of 75/25. The calculations were performed using curves as those presented in Figures 2 and 3.

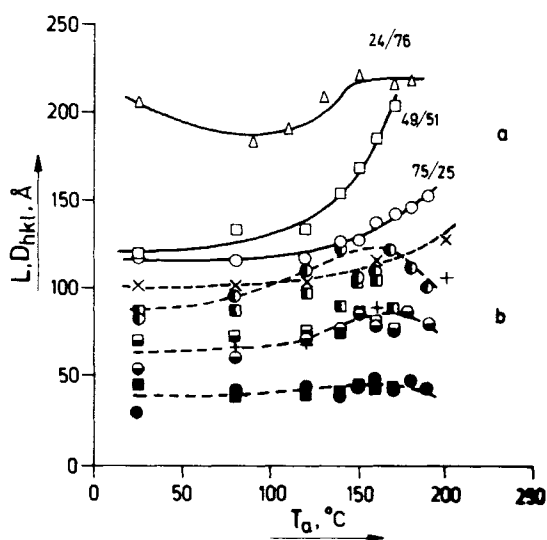


FIGURE 5 Effect of the annealing temperature  $T_a$  on the long spacing  $L$  (a) and crystallite size  $D_{hkl}$  (b) for undrawn PBT and PEE with various PBT/PEG(1000) ratios (wt.%): ( $\Delta$ ) -  $L$  of 24/76(1000), ( $\square$ ) -  $L$  of 49/51(1000), ( $\circ$ ) -  $L$  of 75/25(1000); ( $\blacksquare$ ) -  $D_{104}$ , ( $\blacksquare$ ) -  $D_{100}$ , ( $\blacksquare$ ) -  $D_{010}$  of 49/51(1000); ( $\bullet$ ) -  $D_{104}$ , ( $\bullet$ ) -  $D_{100}$ , ( $\bullet$ ) -  $D_{010}$  of 75/25(1000); ( $\blacktriangledown$ ) -  $D_{010}$ , ( $+$ ) -  $D_{100}$  of 100/0. The calculations were performed using curves as those presented in Figures 2 and 3.

are even better expressed (Figure 5). The initial  $L = 120 \text{ \AA}$  in samples 75/25(1000) and 49/51(1000) increases in the annealing range 120–170°C by 20 and 80%, respectively. In the same temperature interval the crystallite sizes in the (100) and (010) directions increase steadily by only about 20–30% for both samples. What is more, sample 75/25(1000) distinguished by higher melting temperature ( $T_m^{\max} = 212^\circ\text{C}$  against  $T_m^{\max} = 188^\circ\text{C}$  for sample 49/51(1000), Table I) shows a drop in the crystallite size in both directions at  $T_a = 170^\circ\text{C}$  and higher (Figure 5b). This trend is slightly expressed in the case of drawn samples (( $\bar{1}04$ ) direction, Figure 4b) while the crystallite size in the same direction remains unaffected by  $T_a$  for both compositions in the isotropic state (Figure 5b). In this case the average dimension of the intercrystalline amorphous regions  $l_a = L - D_{hkl}$  looks to remain almost constant up to  $T_a$  of about 120°C (for sample 75/25(1000) up to 170°C) and thereafter increases rapidly, almost doubling its initially constant value. Such a change in  $l_a$  means that in this annealing range where the drastic increase of  $L$  takes place, crystal thickening does not contribute to the rise of the long spacing. Because of the importance of  $l_a$  its behavior will be discussed in detail later when its values for both drawn and undrawn samples will be presented as a function of  $T_a$ .

This conclusion is supported also in the case of the lowest hard segment content (Figure 5a, sample 24/76(1000)). At least three striking observations should be noted: (i) this sample displays the highest  $L$ -values although it is characterized by the lowest PBT content; (ii)  $L$  increases regardless of the fact that almost no crystalline phase can be detected by WAXS, (Figure 2b) in accordance with our<sup>19</sup> and other<sup>5</sup> previous observations; (iii) the long spacing reaches a constant value at the highest annealing temperatures some of which are even higher than  $T_m^{\max}$  of the semicrystalline sample 49/51(1000) (Figure 5a, Table I). The behavior of sample 24/76(1000) clearly indicates that not only the increase of the long spacing upon annealing of segmented block copolymers at high temperatures cannot be explained by the phenomenon of crystal thickening but even the appearance of long spacing can have a completely different origin, in contrast to the case of semicrystalline homopolymers.

Comparison of the  $L$ -values obtained with drawn (Figure 4a) and undrawn (Figure 5a) PEE samples leads to the conclusion that the isotropic samples exhibit higher  $L$ -values at the same annealing temperatures and durations similarly to the case of homopolymers.<sup>2,21</sup>

These differences in the behavior of drawn and undrawn PEE with various PBT/PEG(1000) ratios are well expressed in Figure 6. In this connection an important question arises: to what extent the generally accepted explanation for homopolymers<sup>21</sup> is applicable to segmented block copolymers. An attempt to answer this question is made below.

The results presented in Figures 2–6 refer to samples differing in chemical composition, i.e. samples having various PBT/PEG ratios but always containing soft segments of the same length (PEG 1000). Our previous<sup>13–19,22</sup> and present results indicate the determining role of the amorphous regions in the formation of the  $L$ -values. For this reason more systematic experiments with soft segments differing in their length (PEG 600, PEG 1000 and PEG 2000) were carried out.

Figure 7 shows the SAXS curves of undrawn (a) and drawn (b) PEE differing

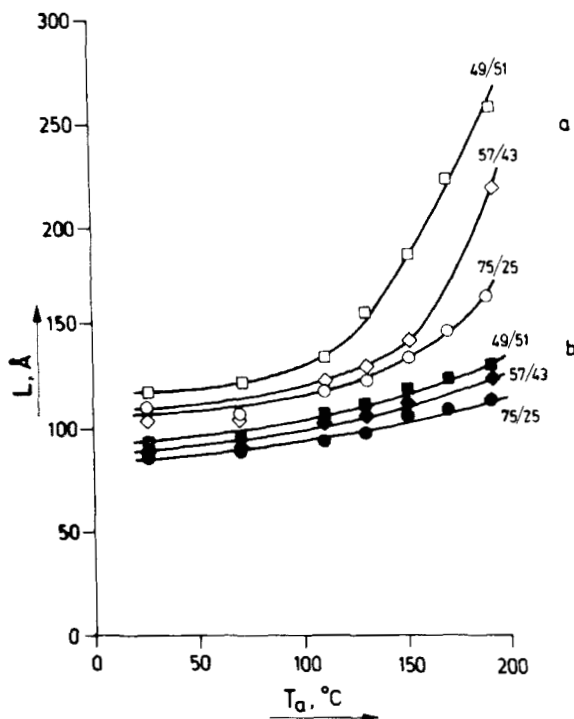


FIGURE 6 Effect of the annealing temperature  $T_a$  on the long spacing  $L$  for undrawn (a) and drawn (b) PEE with various PBT/PEG(1000) ratios (wt. %): ( $\square$ ,  $\blacksquare$ ) - 49/51(1000), ( $\diamond$ ,  $\blacklozenge$ ) - 57/43(1000), ( $\circ$ ,  $\bullet$ ) - 75/25(1000).<sup>14</sup>

in both chemical composition and soft segment length. Similar curves were taken with undrawn samples annealed at various temperatures and the tendency observed in Figure 7a concerning the effect of the soft segment length was preserved in this case, too. The dependence of the small angle peak intensity on the PEG length ( $\bar{M}_n^s$ )<sup>1/2</sup> is shown in Figures 8a and 8b for undrawn annealed and drawn unannealed samples, respectively. The results plotted in Figure 8 lead to two important conclusions: (i) the drawn samples (Figure 8b) show a peak intensity lower down to one order of magnitude than that of the undrawn ones (Figure 8a) at the same chemical composition and annealing temperature; (ii) the longer the soft segments, the stronger the effect of  $T_a$  on the peak intensity is (Figure 8a). This last conclusion means that the density difference between the crystalline and non-crystalline regions increases with the temperature. Taking into account the fact that during annealing only a slight increase of the crystalline density can be expected due to perfection processes, the strong rise of the density difference can be explained only by a drastic expansion (dilution) of the amorphous regions with  $T_a$ . This effect is the stronger, the higher the  $\bar{M}_n^s$ -value is (Figure 8a).

In the case of drawn samples with much more regular structure distinguished by microfibrils and alternating lamellae interconnected by numerous tie-molecules the freedom of expansion is quite limited and thus the dilution effect is much smaller.

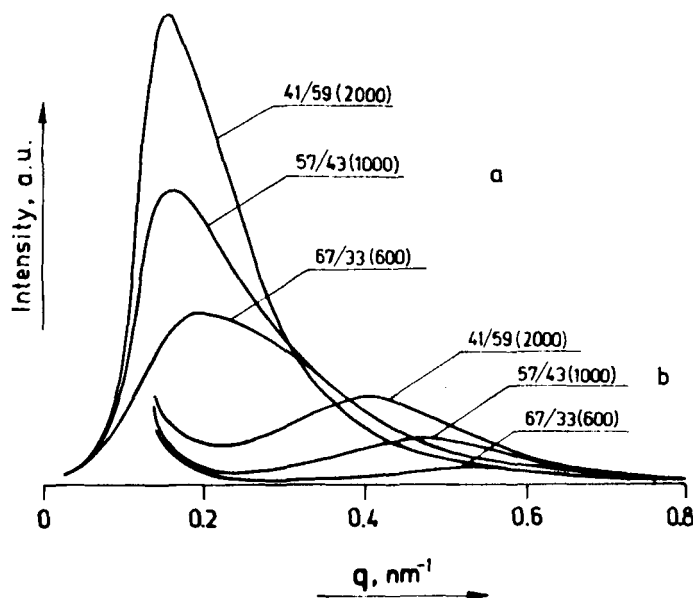


FIGURE 7 SAXS curves of undrawn (a) and drawn (b) PEE bristles with various chemical composition and soft segment length as indicated to the respective curves;  $q = (2\pi \sin \theta)/\lambda$ . The measurements are carried out using a rotating anode and two-dimensional position-sensitive detector.

For this reason the observed scattering intensity changes are insignificant (Figure 8b).

Figures 9a and 9b show the long spacing (calculated from the curves as those of Figure 7) vs.  $(\bar{M}_n^s)^{1/2}$  for annealed drawn and undrawn samples, respectively. They confirm the above observations concerning the changes of  $L$ .

Extrapolation to zero PEG content of the  $L$ -values of drawn annealed (Figures 9b) samples leads to  $L$  of about 50 Å. It is interesting to note here that this value corresponds to the average lamella thickness  $l_c$  in the drawn PEE bristles regardless of the chemical composition (Figure 4b, Reference 16). The same extrapolation for undrawn annealed samples (Figure 9a) indicates a value of about 105 Å which should correspond to the average crystallite size in the sample annealed at  $T_a = 150$ – $180^\circ\text{C}$  and free of PEG, i.e. homo-PBT. Previous WAXS measurements of the crystallite size in homo-PBT,<sup>23</sup> as well as the present studies of the undrawn sample 75/25(1000), plotted together in Figure 5 demonstrate that the crystallite size in the (010) direction at crystallization temperatures in the range 150– $180^\circ\text{C}$  is in the vicinity of 100 Å.

The values of  $l_c$  and  $\bar{D}_{hkl}$ , (averaged from  $D_{100}$ ,  $D_{010}$  and  $D_{104}$ ), provide some idea about the contribution of the crystalline phase to the formation of the long spacing  $L$  in drawn and undrawn samples. The difference  $l_a = L - l_c$  or  $l_a = L - \bar{D}_{hkl}$  determines the dimension of the intercrystalline amorphous regions for drawn and isotropic material, respectively. The effect of the annealing temperature  $T_a$  on the two constituents of the long spacing—the intercrystalline dimension  $l_a$  and crystallite size  $\bar{D}_{hkl}$  (or  $l_a$  and  $l_c$  for the case of drawn samples) is shown in Figure 10a and Figure 10b for undrawn and drawn material, respectively. Since the

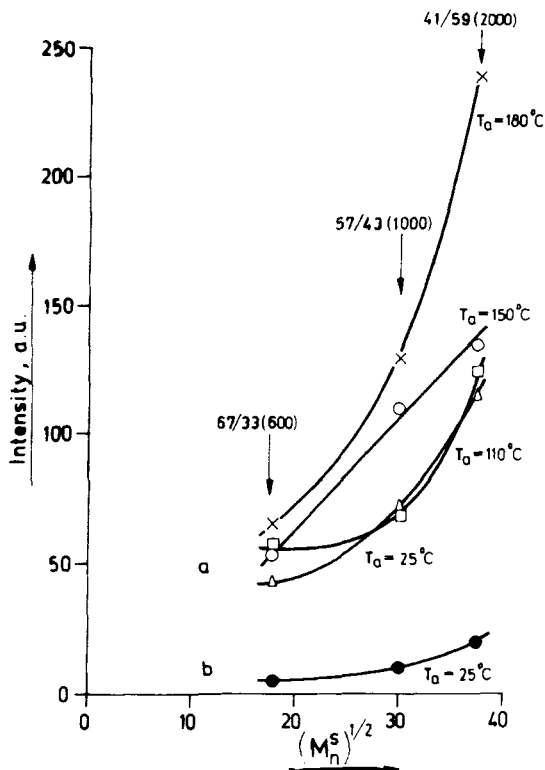


FIGURE 8 Dependence of the SAXS peak intensity  $I$  on the square root of the number average molecular weight of soft segments  $(M_n^S)^{1/2}$  for undrawn (a) and drawn (b) samples with various chemical composition and annealing temperature as indicated as follows: ( $\bullet$ ,  $\Delta$ ) -  $T_a = 25^\circ\text{C}$ ; ( $\square$ ) -  $T_a = 110^\circ\text{C}$ ; ( $\circ$ ) -  $T_a = 150^\circ\text{C}$  and ( $\times$ ) -  $T_a = 180^\circ\text{C}$ . The data are taken from curves as those presented in Figure 7.

crystallite size remains almost unchanged (Figures 4b and 5b) within the entire  $T_a$  range, the drastic increase of  $L$  with  $T_a$  (Figures 4a, 5a and 9) can originate solely from the rise in the dimension of  $l_a$ .

## DISCUSSION

### Does Crystal Thickening Exist in Segmented Polyblock Copolymers?

The answer to this question is the primary task of the present study. As already pointed out, the phenomenon of crystal thickening in semicrystalline homopolymers<sup>2</sup> was adopted in order to explain the strong increase of the long spacing with crystallization temperature in segmented polyblock copolymers.<sup>1,8,10</sup> In the same time indications exist<sup>11</sup> that this explanation is not a universal one. Our previous measurements demonstrated that blocks with very short length can restrict crystal thickening at least in the "c"-direction in drawn materials.<sup>16,18</sup> For this reason the change in the long spacing and crystallite size was followed directly by SAXS and

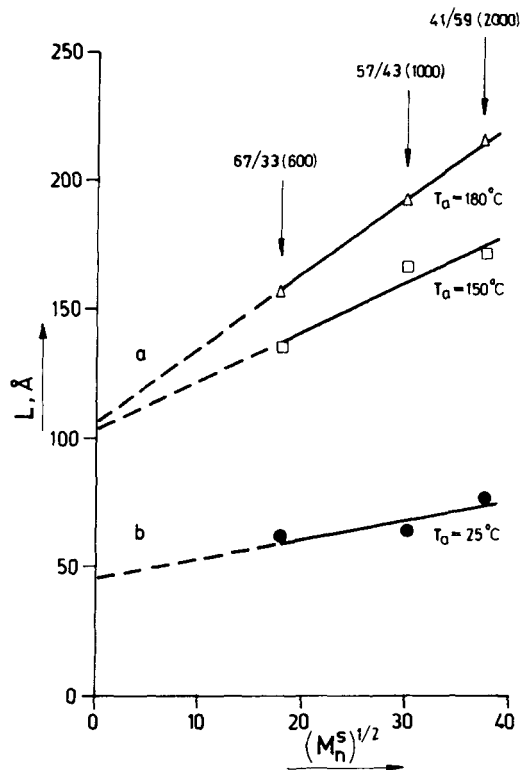


FIGURE 9 Dependence of the long spacing  $L$  on the square root of the number average molecular weight of soft segments  $(M_n^s)^{1/2}$  for undrawn (a) and drawn (b) samples with various chemical composition and annealing temperature as indicated as follows: ( $\bullet$ ) -  $T_a = 25^\circ\text{C}$ ; ( $\square$ ) -  $T_a = 150^\circ\text{C}$  and ( $\Delta$ ) -  $T_a = 180^\circ\text{C}$ . The data are taken from curves as those presented in Figure 7.

WAXS as dependent on the crystallization temperature in the case of PEE differing in their PBT/PEG ratio (Figures 4 and 5). Further, in order to demonstrate the dominating role played by the intercrystalline amorphous regions in the formation of the long spacing, the effect of the soft segment length  $l^s$  on  $L$  was studied for various annealing temperatures (Figure 9).

The results obtained lead to several conclusions. The situation with oriented bristles is much clearer (Figure 4). Direct measurements of the lamellae thickness by WAXS for two samples (75/25(1000) and 49/51(1000)) show that  $l_c$  varies between 50 and 60 Å within the entire annealing range in agreement with previous measurements on samples with a larger variety in their PBT/PEG ratio.<sup>16</sup> This rather constant value of  $l_c$  suggests the lack of crystal thickening in the samples studied (Figure 4b,<sup>16</sup>). It should be noted that in the case of sample 49/51 (1000) this could be due to the very short hard segments ( $l^h = 51$  Å, Figure 1, Table I). However, sample 75/25(1000) has  $l^h = 160$  Å (Figure 1, Table I); obviously, in this second case the absence of crystal thickening is related to the copolymer nature of the macrochains—the presence of non-crystallizable blocks restricts the recrystallization ability of the hard segments due to the large number of inter- and

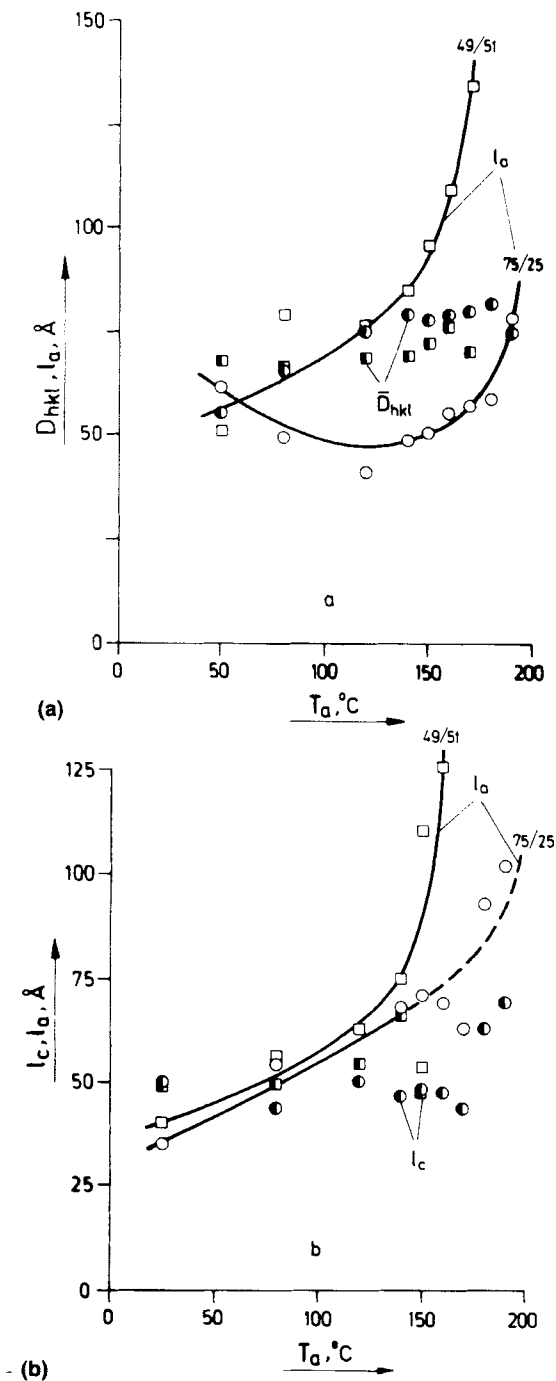


FIGURE 10 Effect of the annealing temperature  $T_a$  on the intercrystalline amorphous areas dimension  $l_a$ , average crystallite size  $\bar{D}_{hkl}$  of undrawn (a) and lamellae thickness  $l_c$  of drawn (b) PEE samples differing in PBT/PEG(1000) ratio in wt. % as follows: (■, □) - 49/51 and (○, ●) - 75/25.  $\bar{D}_{hkl}$  is averaged from  $D_{010}$ ,  $D_{100}$  and  $D_{104}$ .

intrafibrillar tie-molecules as demonstrated recently on the same drawn samples by following their deformation ability using SAXS.<sup>17,18</sup>

The observed increase of the long spacing by 80% at higher annealing temperatures (Figure 4a) can be thus explained solely by the volume changes in the non-crystalline interlamellar regions consisting of soft and hard segments.<sup>16–18</sup> This conclusion is supported also by the fact that the longer the soft segments, the higher and more temperature sensible the long spacings are as reported by Wegner<sup>11</sup> and observed in the present study (Figures 4a and 5a).

The same general conclusion concerning the nature and temperature dependence of the long spacing in PEE can be drawn from the measurements on undrawn samples, too (Figure 5). Although in this particular case crystal thickening of about 20–30% can be observed in the (100) and (010) directions (Figure 5b), it is by far not enough so as to explain the rise in  $L$  by 80% for sample 49/51(1000) (Figure 5a). It is interesting to note here that the long spacing of the richest in PBT sample 75/25(1000) follows rather accurately the increase in the crystallite sizes  $D_{010}$  and  $D_{100}$  of homo-PBT (sample 100/0) up to  $T_a = 190^\circ\text{C}$  in contrast to the sizes in the same directions of sample 75/25(1000) which drop at  $T_a$  higher than  $170^\circ\text{C}$ , approaching their starting values and demonstrating in this way some “negative” crystal thickening. This means again that precisely at the highest annealing temperatures, i.e. under the most favorable crystallization conditions, the increase in  $L$  cannot be related to crystal thickening.

The best proof in favor of this statement is the observation of long spacing even in PEE free of crystalline phase (Figures 2b and 5a, sample 24/76(1000)). This interesting observation was reported earlier by Perego et al. for a similar PEE system.<sup>5</sup> Their studies show that, unlike semicrystalline homopolymers, the appearance of a peak in the SAXS curves can have a completely different origin. As shown by our earlier studies<sup>19</sup> the existence of long spacing in the absence of crystalline phase is related to the multiphase character of the systems under investigation. The rise of  $L$  with  $T_a$  for such samples is due to dephasing processes as proved for PEE based on PBT and PEG by means of synchrotron radiation.<sup>19</sup>

The measurements on isotropic samples support earlier results<sup>11,14</sup> that the higher the soft segment content, the longer the long spacing is (Figure 5a).

The predominant contribution of the amorphous intercrystalline regions to the formation of the long spacing and the strong temperature dependence of the latter are best illustrated by the measurements on samples containing soft segments of different length (Figures 7–9). It is seen in Figure 9 that the longest soft segments result in the highest and most temperature-dependent long spacing (Figure 9a). The variations in the  $L$ -values up to 150% resulting from the PBT/PEG ratio, PEG molecular weight and thermal treatment when the crystallite size remains almost constant are related solely to volume increase of the amorphous regions. Usually this volume change is accompanied by dilution effects leading to a rise in the density difference between ordered and disordered regions as demonstrated by the SAXS curves (Figures 7 and 8).

Finally some comments on the question how reasonable is the plotting in Figure 9 of the results for samples containing three PEG of different molecular weights (600, 1000 and 2000, Table I). All above considerations lead to the general con-



clusion that the only reason for the changes in the long spacing with the glycol molecular weight should be the change in the size of the amorphous regions. If we assume, somewhat arbitrarily, a random coil conformation of the soft segments, then their size, taken as the root mean square unperturbed end-to-end distance will be proportional to  $(M_n^s)^{1/2}$ .<sup>24</sup> Taking into account that the molecular weights of the two fractions are 1400 and 380 (Table I), the size of the coils of the longer molecules will be  $(1400/380)^{1/2} = 1.9$  times bigger than the respective size of the shorter molecules coils. If we assume further that the bigger coils are densely packed, then the smaller coils may be situated between them and this will not affect the size of the amorphous regions which will be determined by the bigger coils. Thus it seems reasonable to attribute the observed long spacing with samples containing PEG 2000 to number average molecular weight 1400 rather than 380.

Concerning the drawn samples (Figure 9b) it should be taken into account that the values of  $l_a = L - l_c$  for the three different glycols used are roughly 15, 20 and 25 Å, respectively. Taking into account that  $L_{\max} = l_c + 2l^s + l^h$  and  $l_a = 2l^s + l^h$  according to our previous studies<sup>16-18</sup> the numerical values of  $l_a$  for the three samples studied (Figure 9b) are 100, 190 and 180 Å, respectively (Table I), i.e. they are about ten times higher than the measured ones (Figure 9b). It should be noted that the  $l_a$ -values are even slightly higher when they are derived from the experimentally measured maximum values of  $L$ , i.e.  $l_a = L_{\max} - l_c$ .<sup>16</sup> Thus the conformation of the chains in the interlamellar amorphous regions is quite far from the completely extended one and much closer to a coil hence the plotting for drawn samples looks rather reasonable.

The last argument in favor of the plotting in Figure 9 is the very good agreement between the values of the lamellae thickness  $l_c$  and the crystallite sizes  $D_{hkl}$  obtained through extrapolation of only three points (Figure 9) and direct measurements by WAXS (Figures 4b, 5b and Reference 16). The same approach was already used by Fischer et al. for polyblock polyurethans distinguished by monodisperse hard segment length and PTMO of molecular weight of 650, 1000 and 2000.<sup>25</sup> Their extrapolation based again on three points yielded  $l_c = 55$  Å which corresponds to the crystallite size in the "c"-direction of the hard segments determined by WAXS on model substances by Blackwell et al.<sup>26,27</sup>

The components of the long spacing ( $l_c$  or  $\bar{D}_{hkl}$  and  $l_a$ ) for PEE differing in chemical composition and their  $T_a$ -dependence are plotted in Figures 10a and 10b, illustrating in the best way that the most temperature-sensitive component of  $L$  is the amorphous part  $l_a$  rather than the crystalline one. Since crystallites are almost insensitive to the rise of  $T_a$  (Figures 10a and 10b), the conclusion can be drawn that the repeatedly observed strong increase of the long spacing with temperature for segmented polyblock copolymers originates from the expansion of the intercrystalline amorphous regions and, in contrast to the case of semicrystalline homopolymers, it is not related to the phenomenon of crystal thickening.

### Effect of Temperature on the Long Spacing in the Isotropic and Oriented State

The general dependence of  $L$  on  $T_a$  can be seen in Figures 4a, 5a, 6 and 9. Particularly Figure 6 clearly shows that the copolymers behave in general as those based on PBT and PTMO<sup>11</sup> as well as the typical semicrystalline homopolymers—

again it should be noted that the long spacings are much higher in the case of undrawn samples (Figure 6a) than those of drawn ones (Figure 6b) crystallized at the same temperature. This effect has been observed with both homopolyesters—PBT<sup>4</sup> and PET<sup>3</sup>—and is explained by the influence of stress or strain on the melting point and the dependence (according to the kinetic theory of crystallization) of  $L$  on the supercooling.<sup>28</sup> Flory showed that the polymer elongation leads to an increase of the free energy and therefore the melting temperature of the crystallites and the supercooling is increased.<sup>29</sup> Then at constant crystallization temperature a decrease in  $L$  is expected with an increase of orientation. Theoretical interpretations of this effect were proposed by Kobayashi<sup>30</sup> and by Krigbaum.<sup>31</sup> It seems, however, that the observed difference in the  $L$  values between drawn and undrawn samples is rather large compared to that of homopolymers<sup>3</sup> and probably is not due only to crystallization kinetics.

The second peculiarity of the curves discussed (Figure 6) is the very high sensitivity of the  $L$ -values to the annealing temperatures in the case of undrawn samples with low PBT content (49 and 57 wt. %, Figure 6). The two-fold increase of  $L$  can be explained only by an intensive phase separation process (dephasing) at high  $T_a$  and formation of amorphous PEG regions with increasing dimensions. Commenting on the crystallization behavior of PEE, Briber and Thomas<sup>33</sup> conclude that the thickness of the amorphous layers should be directly proportional to the soft segment content of the sample. The length differences of the hard blocks participating in crystallization suppose diffuse crystal boundaries. This conclusion disagrees with that of Bandara and Droscher<sup>3</sup> who suggest sharp boundaries starting from their SAXS studies. It is found by Zhu *et al.*<sup>34</sup> that a similar SAXS behavior is shown by PEE based on PBT and PTMO crystallized from the melt at different temperatures. An increase of  $L$  due to the rise of the content of amorphous regions (with simultaneous decrease of the degree of crystallinity) has been reported for PET containing chemically bonded  $-\text{OCH}_2\text{CH}_2\text{OCH}_2\text{CH}_2\text{O}-$ units.<sup>35</sup>

In addition to experiments with synchrotron radiation,<sup>19</sup> proofs in favor of dephasing of amorphous PBT and PEG blocks with the rise of temperature can be found in the results of DSC measurements on the same samples.<sup>14</sup> The sample with the lowest PEG content (75/25(1000)) is of particular interest since it demonstrates a drastic effect of  $T_a$  on  $T_g^{\text{PEG}}$  ( $T_g^{\text{PEG}}$  drops with  $T_a$  from  $-17^\circ\text{C}$  to  $-43^\circ\text{C}$  in the case of undrawn samples and from  $-28^\circ\text{C}$  to  $-43^\circ\text{C}$  for drawn ones).<sup>14</sup> The unannealed sample contains two amorphous phases—pure PBT and another one consisting of PBT and PEG segments with  $T_g^{\text{PBT+PEG}}$  situated between  $T_g^{\text{PBT}}$  and  $T_g^{\text{PEG}}$ .<sup>14</sup> This second phase undergoes phase separation at higher temperatures resulting in basically homogeneous amorphous phases distinguished by their  $T_g^{\text{PBT}}$  and  $T_g^{\text{PEG}}$ . Thus, the dependence of  $T_g$  on  $T_a$  and on the chemical composition supports the conclusion about dephasing with increasing temperature.

In the same time the increase of  $L$  in the case of drawn samples is only 30% (Figure 6b) which is rather low compared to that of the undrawn ones with the same chemical composition (about 100%, Figure 6a). This difference between drawn and undrawn samples with respect to the effect of  $T_a$  on  $L$  could be explained by the fact that orientation restricts further dephasing and the formation of amor-

phous PEG regions with large dimensions is hindered as supported by the changes of  $T_g^{PBT}$  for both types of samples cited above.<sup>14</sup>

The basic contribution of the amorphous phase to the formation of  $L$  and the high temperature-sensitivity of the latter (particularly in the isotropic state) is demonstrated by SAXS measurements on samples differing in soft segment length (PEG 600, PEG 1000 and PEG 2000, Figures 7–9). The samples containing PEG 2000 show not only the highest  $L$  values (Figure 9) and the strongest SAXS intensity (Figure 8) but also the largest relative increase in  $L$  as a result of annealing under the same conditions (Figure 9).

Finally, discussing the effect of annealing on the long spacing of PEE in the oriented and isotropic state, the following consideration should be taken into account. There are sufficient reasons, particularly in the case of polyblock copolymers characterized by polydisperse hard segment lengths, for the formation of crystallites strongly differing in their size and perfection. For obvious reasons this situation should be better expressed in the case of undrawn materials. The variety in crystallite perfection and size will lead to different melting ranges. At certain temperatures some of the crystallites will disappear increasing effectively in this way the distance between the remaining crystallites and hence the  $L$ -values. Such a partial melting was assumed by Koberstein *et al.*<sup>36</sup> who followed the morphological changes during scanning in the calorimeter of a polyurethane elastomer. Thus, in addition to the phase separation in the amorphous regions, the effectively disappearing of the more defective crystallites with the rise of  $T_a$  contributes substantially to the drastic increase of  $L$  in the isotropic state.

This effect was recently demonstrated using the same samples as in the present study even in the drawn state.<sup>18</sup> By means of thermal treatment and/or additional drawing two types of crystalline lamellae differing in their perfection are created. Subsequent annealing and/or extension during SAXS measurements lead to a density value of the less perfect lamellae which can be closer to that of the more perfect lamellae or closer to the amorphous regions. In the second case a drastic (two-fold) increase of the  $L$ -value is observed.<sup>18</sup>

Summarizing the results and discussions concerning the effect of the annealing temperature and chemical composition on the scattering and thermal behavior of the studied poly(ether ester)s it can be concluded that there are clear evidences for phase separation of the amorphous soft and hard segments favored by the increase of the annealing temperature. This separation, together with the pre-melting of the less perfect and smaller crystallites, provides a reasonable explanation of the SAXS results—a stronger increase of both the long spacing and the scattering power with the rise of  $T_a$  in the case of less crystalline and undrawn copolyesters.

## CONCLUSIONS

On the basis of detailed WAXS and SAXS measurements on annealed drawn and undrawn PEE differing in both PBT/PEG ratio and PEG molecular weight and comparing the results with previous ones obtained with similar systems, the following conclusions can be drawn:

1. The well known strong dependence of  $L$  on  $T_a$  is confirmed but it cannot be explained by the phenomenon of crystal thickening generally accepted for homopolymers because: (i) the lamellae thickness  $l_c$  (for drawn samples) and crystallite size  $D_{hkl}$  (for undrawn samples) remain almost constant with the rise of  $T_a$ ; (ii)  $L$  drops with the increase of crystallizable segments content in PEE and (iii)  $L$  is most sensitive to  $T_a$  in samples with the highest molecular weight of PEG.

2. The increase of  $L$  with  $T_a$  is explained by the expansion of the amorphous intercrystalline regions as a result of different factors.

3. The usually observed higher values of  $L$  for undrawn samples cannot be explained solely by differences in the crystallization kinetics as in the case of homopolymers. Another peculiarity of the copolymers should be taken into account as their multiphase nature leads to dephasing processes and premelting of less perfect crystallites. Both processes—dephasing and premelting are strongly hindered in the drawn state and therefore they contribute to a lesser extent to the increase in  $L$  with  $T_a$  than in the case of isotropic material.

4. The conclusions drawn from the results of the present study seem to be applicable to other segmented polyblock copolymers distinguished by similar scattering and thermal behavior.

### Acknowledgment

C. Fakirov gratefully acknowledges the hospitality of Max-Planck Institut fuer Polymerforschung, Mainz, where a part of the experiments were carried out in the frame of the Governmental Agreement for Scientific and Technical Cooperation between Republic of Bulgaria and the Federal Republic of Germany.

### References

1. *Thermoplastic Elastomers—A Comprehensive Review*, N. R. Legge, G. Holden and H. E. Schroeder (Eds.), Hanser Publishers, Munich, Vienna, New York, 1987.
2. B. Wunderlich, *Macromolecular Physics*, Vol. 2, Academic Press, New York, San Francisco, London, 1976.
3. E. W. Fischer and S. Fakirov, *J. Mater. Sci.*, **11**, 1041 (1976).
4. S. Fakirov and A. Alexandrov, *Compt. rend. Bulg. Acad. Sci.*, **10**, 598 (1977).
5. G. Perego, M. Cesari and R. Vitali, *J. Appl. Polym. Sci.*, **29**, 1157 (1984).
6. W. H. Buck, R. J. Cella, E. K. Gladding and J. R. Wolfe, Jr., *J. Polym. Sci. Symp.*, **48**, 47 (1974).
7. G. Wegner, T. Fujii, W. Meyer and G. Lieser, *Angew. Makromol. Chem.*, **74**, 295 (1978).
8. R. K. Adams and G. K. Hoeschele, Thermoplastic Polyester Elastomers, in: Reference 1.
9. H. Schroeder and R. Cella, Polyesters, Thermoplastic, in: *Encyclopedia of Polymer Science and Engineering*, Vol. 12, John Wiley & Sons, New York, 1988.
10. J. A. Miller and S. L. Cooper, Chain Conformation in Block Copolymers by Small Angle Neutron Scattering, in: Reference 1.
11. G. Wegner, Model Studies Toward a Molecular Understanding of the Properties of Segmented Block Copolyetheresters, in: Reference 1.
12. S. Fakirov and T. Gogeva, *Makromol. Chem.*, **191**, 603 (1990).
13. *Ibid.* **191**, 615 (1990).
14. *Ibid.* **191**, 2341 (1990).
15. *Ibid.* **191**, 2355 (1990).
16. A. A. Apostolov and S. Fakirov, *J. Macromol. Sci. Phys.*, in press.
17. S. Fakirov, C. Fakirov, E. W. Fischer and D. Stamm, *Polymer*, **32**, 1173 (1991).
18. S. Fakirov, C. Fakirov, E. W. Fischer and D. Stamm, *Polymer*, in press.

19. S. Fakirov, A. A. Apostolov, P. Boeseke and H. G. Zachmann, *J. Macromol. Sci. Phys.*, **B29**, 3779 (1990).
20. H. P. Klug and L. E. Alexander, *X-Ray Diffraction Procedures for Polycrystalline and Amorphous Materials*, John Wiley & Sons, New York, 1974, p. 511.
21. S. Fakirov, *Structure and Properties of Polymers*, Sofia Press, Sofia, 1985 (distributed by Martinus Nijhoff, Int., Holland).
22. S. Fakirov, *Polymer*, **21**, 373 (1980).
23. I. Seganov, S. Fakirov, M. Krasteva and V. Krastev, *Bulg. J. Phys.*, **8**, 179 (1981).
24. D. W. Van Crevelen, *Properties of Polymers*, Elsevier, Amsterdam, 1972, p. 249.
25. E. W. Fischer and U. Struth, unpublished data; U. Struth, PhD Thesis, University of Mainz, Mainz, 1986.
26. J. Blackwell and K. H. Gardner, *Polymer*, **20**, 13 (1979).
27. J. Blackwell and M. R. Nagarajan, *Polymer*, **22**, 202 (1981).
28. L. Mandelkern, *Crystallization of Polymers*, McGraw-Hill, New York, 1964.
29. P. J. Flory, *J. Am. Chem. Soc.*, **78**, 5222 (1956).
30. K. Kobayashi and T. Nagasawa, *J. Macromol. Sci. Phys.*, **B4**, 331 (1970).
31. W. K. Krigbaum and R. J. Roe, *J. Polym. Sci., Part A*, **2**, 4391 (1964).
32. R. M. Briber and E. L. Thomas, *Polymer*, **26**, 8 (1985).
33. U. Bandara and M. Droscher, *Colloid Polym. Sci.*, **261**, 26 (1983).
34. L.-L. Zhu, G. Wegner and U. Bandara, *Makromol. Chem.*, **182**, 3639 (1981).
35. S. Fakirov, I. Seganov and E. Kurdova, *Makromol. Chem.*, **182**, 185 (1981).
36. J. T. Koberstein and T. P. Russell, *Macromolecules*, **19**, 706 (1986).